Available online at www.sciencedirect.com

ScienceDirect

Advances in Space Research 58 (2016) 2126–2133

ADVANCES IN SPACE RESEARCH (a COSPAR publication)

www.elsevier.com/locate/asr

Magnetic fluctuations in anisotropic space plasmas: The effect of the plasma environment

J.A. Valdivia [a,f,*], B.A. Toledo [a], N. Gallo [a], V. Muñoz [a], J. Rogan [a,f], M. Stepanova [b], P.S. Moya [a,d,e], R.E. Navarro [c], A.F. Viñas [d], J. Araneda [c], R.A. López [a], M. Díaz [g]

[a] Departamento de Física, Facultad de Ciencias, Universidad de Chile, Santiago, Chile
[b] Departamento de Física, Facultad de Ciencias, Universidad de Santiago, Santiago, Chile
[c] Departamento de Física, Universidad de Concepción, Concepción 4070386, Chile
[d] NASA Goddard Space Flight Center, Heliophysics Science Division, Geospace Physics Laboratory, Mail Code 673, Greenbelt, MD 20771, USA
[e] Department of Physics, Catholic University of America, Washington, D.C. 20064, USA
[f] Centro para el Desarrollo de la Nanociencia y la Nanotecnología, CEDENNA, Santiago, Chile
[g] Departamento de Ingeniería Eléctrica, Facultad de Ciencias Físicas y Matemáticas, Universidad de Chile, Santiago, Chile

Received 1 June 2015; received in revised form 29 March 2016; accepted 20 April 2016
Available online 28 April 2016

Abstract

The observations in the solar wind, which are usually organized in a beta-anisotropy diagram, seem to be constrained by linear instability thresholds. Unexpectedly, under these quasi-stable conditions, there is a finite level of electromagnetic fluctuations. A relevant component of these fluctuations can be understood in terms of the electromagnetic fields produced by the thermal motion of the charged particles. For the simple case of parallel propagating fields in an electron–proton plasma, we study the effect of the parameter ω_{pp}/Ω_e that characterizes the different space physics environments, and can affect the continuum spectrum produced by these fluctuations, which in turn may be used to understand the relevance of these processes occurring in a specific plasma environment.

Keyword: Thermally induced electromagnetic fluctuations

1. Introduction

Collisionless plasmas, such as the solar wind (Marsch and Goldstein, 1983), can often remain for a long time in a state where collisions cannot generally ensure local thermodynamic equilibrium. In this quasi-stable state, when the effect of instabilities can be disregarded, charge particles move in a random fashion consistent with a thermal distribution, and generate electromagnetic fields. At the same time, and due to the quasi-stable condition of the plasma, the system tries to damp these fields, reaching a finite level that can be generally estimated from a suitable Fluctuation–Dissipation Theorem, as suggested in a number of publications (Callen and Welton, 1951; Ichimaru, 1962; Sitenko, 1967). Researchers have realized that the study of these thermally induced electromagnetic fluctuations (TIEF) can be used to estimate relevant information about the plasma state (Sentman, 1982; Meyer-Vernet et al., 1986, 2000; Lund et al., 1994; Issautier et al., 2001; Moncuquet et al., 2005; Chapman and Gericke, 2011; Li and Hazeltine, 2006) proving to be one of the most efficient methods for plasma diagnostics.

At the same time, it is common in these collisionless space plasma environments with background magnetic

* Corresponding author at: Departamento de Física, Facultad de Ciencias, Universidad de Chile, Santiago, Chile. Tel.: +56 (2) 29787276; fax: +56 (2) 22712973.
E-mail address: alejo@macul.ciencias.uchile.cl (J.A. Valdivia).

http://dx.doi.org/10.1016/j.asr.2016.04.017
0273-1177/

fields, such as the solar wind, that the distribution function of the particle velocity becomes anisotropic, that in a first approximation can be characterized by a parallel temperature ($T_\parallel$) that is usually different from the perpendicular temperature ($T_\perp$), even at 1 AU (Kasper et al., 2008). In this approximation, the anisotropy, which can be defined as $A = T_\perp/T_\parallel$, provides a source of free energy that can sometimes evolve through instabilities (Sagdeev and Shafranov, 1960; Davidson and Ogden, 1975; Weibel, 1959). With these definitions, it is common to organize the solar wind observations in the so called "beta-anisotropy" diagram, where beta (described in detail below) is the ratio between the local thermal and magnetic energy densities. In this diagram it is observed that a large fraction of the solar wind data at 1 AU is usually restricted below the linear instability thresholds (Kasper et al., 2002; Hellinger et al., 2006; Štverák et al., 2008). Hence, most of the plasma, even those situations with relatively large anisotropies, seems to be in a quasi-stable state, with an instability growth rate that is small compared with the collisions and expansion time scales.

However, the data also shows a finite electromagnetic fluctuation level (Bale et al., 2009), which linear theory has trouble explaining because of the finite damping rate. Initially it was suggested that we could be observing the latest stages of the evolution of a previously unstable plasma (Gary et al., 1994, 1998; Seough et al., 2013) or the stabilization of an unstable situation due to propagation effects (Camporeale et al., 2010). It is difficult to account for how an unstable plasma could evolve to a situation that may be quite removed from the instability thresholds. Another possibility is that these fluctuations may be due to remnant MHD turbulent magnetic fluctuations advected from the Sun. For example, Bruno et al. (2001) suggested that the satellites were observing advected entangled flux tubes, with fluctuations becoming more intermittent when the detector crosses the boundary between tubes. Hence, the solar wind observations would be a combination of waves and discontinuities where reconnection could occur. These advected structures would then cascade to the kinetic range due to some nonlinear process, as suggested by the measured spectrum of magnetic fluctuations in the solar wind. Of course, the details of how this process would occur are not completely understood (Goldstein et al., 2015).

Here we take an alternative approach and suggest that a large component of these fluctuations can be explained in terms of TIMF that can be estimated through the use of a Fluctuation–Dissipation Theorem that has been properly modified to account for anisotropic plasmas (Navarro et al., 2014). These ideas have been applied to the ion (Araneda et al., 2011; Navarro et al., 2014, 2015) and electron (Viñas et al., 2015) scales. For solar wind plasmas, it was recently demonstrated in Navarro et al. (2014) that a relevant component of these fluctuations in the anisotropic solar wind can be explained by the thermally induced electromagnetic fluctuations produced by the stochastic motion of the particles in quasi-stable plasmas.

In this work, we analyze the properties of the TIEF propagating along a background magnetic field in solar wind (and magnetospheric) like plasmas composed of electrons and protons. Particular emphasis will be placed on the spectrum variation with the particle density and background magnetic field strength, as combined in the ratio of the proton plasma and cyclotron frequencies (defined below), which characterizes the space plasma environment.

2. Theoretical analysis

The TIEF produced in an electron–proton plasma can be derived directly from the Klimontovich equation (Schlickeiser and Yoon, 2012) for a given distribution function of the particle velocities. We will take a slightly different approach, as suggested by Navarro et al. (2014), which generalizes the work of Sitenko (1967) to multi-species anisotropic plasmas. The approach is to introduce the fluctuating current produced by the thermal motion of the charged particles directly into the Vlasov–Maxwell equations, that includes the dispersion current, and use ensemble theory to obtain a TIEF amplitude that is independent of the introduced fluctuating current.

Although the TIEF are usually produced in all directions, we will consider for simplicity the fluctuations that propagate along the background magnetic field $\mathbf{B} = B_0\hat{z}$ in an uniform plasma at the proton scales. We can relate the fluctuating current $\tilde{\boldsymbol{j}}$, generated by the random motion of the charged particles, with the ensemble averaged electric field $\langle \mathbf{E}(k,\omega)\rangle$ through the Fourier transformed Maxwell's equations as

$$\langle \boldsymbol{\Lambda}\mathbf{E}(k,\omega)\rangle = \frac{4\pi}{i\omega}\tilde{\boldsymbol{j}}. \tag{1}$$

Here $\boldsymbol{\Lambda}$ (to be specified below) is the dispersion tensor which depends on the equilibrium particle distribution function F_α for species α. When there is no fluctuating current, this expression corresponds to the dispersion relation obtained from linear theory. The ensemble average of the s component of the fluctuating electric field is given by

$$\langle E_s\rangle = \frac{\sum_\alpha \int dx E_s f_\alpha}{\sum_\beta \int dx f_\beta}, \tag{2}$$

where the integral is done over the phase space x. The distribution function of species α, f_α, depends on the energy of the system $\mathscr{H}$. The ℓ component of the fluctuating current $\tilde{j}_\ell$ produces the perturbation $2i\omega\Delta\mathscr{H}_\ell(\mathbf{k},\omega) = \tilde{j}_\ell E_\ell(\mathbf{k},\omega)$ to the energy, for coordinates $\ell = \{x,y,z\}$, and a change in the distribution function. After expanding Eq. (2) to first order in $\Delta\mathscr{H}_\ell$, we obtain the ensemble averaged perturbed electric field components, given by

$$\langle E_s(\mathbf{k},\omega)\rangle = i\omega\sum_{\alpha,\ell}\langle \Delta\mathscr{H}_\ell(\mathbf{k},\omega)E_s^*(\mathbf{k},\omega)\rangle_\alpha^{(\ell)}, \tag{3}$$

where the asterisk represents a complex conjugate; the double sum extends over all species α and coordinates ℓ, and

$$\langle A\rangle_\alpha^{(\ell)} = \frac{\int dx(\partial F_\alpha/\partial \mathscr{H}_\ell)A}{\sum_\beta \int dx F_\beta}. \quad (4)$$

Combining Eqs. (1) and (3) we obtain

$$\sum_\alpha \langle E_\ell\, E_s^*\rangle_\alpha^{(\ell)} = \frac{8\pi}{i\omega}\Lambda_{s\ell}^{-1}, \quad (5)$$

which needs to be related to the total electric field fluctuations as $\langle E_i\, E_j^*\rangle = \sum_\alpha \langle E_i\, E_j^*\rangle_\alpha$. Notice that Eq. (5) is written explicitly in terms of $\mathbf{\Lambda}^{-1}$, which produces a continuous spectrum for ω and $\mathbf{k}$, with peaks near the normal modes defined by the dispersion relation $\det(\mathbf{\Lambda}) = 0$.

For distribution functions of the form $F_\alpha \propto e^{-\mathscr{H}_\alpha/k_B T_\alpha}$, where $\mathscr{H}_\alpha$ as the Hamiltonian of species α at equilibrium, it is easy to evaluate $\langle E_i\, E_j^*\rangle_\alpha$, since the derivative with respect to $\mathscr{H}_\alpha$ essentially produces $-F_\alpha/k_B T_\alpha$. Here we consider a neutral electron–proton plasma, described by a bi-Maxwellian distribution function for species α ($\alpha = p,\ e$),

$$F_\alpha(v_\perp, v_\parallel) = \frac{1}{\pi^{3/2}u_{\perp\alpha}^2 u_{\parallel\alpha}} \exp\left[-\frac{v_\perp^2}{u_{\perp\alpha}^2} - \frac{(v_\parallel - U_\alpha)^2}{u_{\parallel\alpha}^2}\right], \quad (6)$$

where $u_{\parallel\alpha}^2 = 2k_B T_{\parallel\alpha}/m_\alpha$ and $u_{\perp\alpha}^2 = 2k_B T_{\perp\alpha}/m_\alpha$ are the square of the thermal speeds; k_B is the Boltzmann constant; and U_α is the drift speed. Following Navarro et al. (2014), we can relate the electric field fluctuations

$$\frac{1}{8\pi}\langle |E_\ell|^2\rangle = \sum_\alpha \frac{1}{\omega}\frac{k_B T_{\ell\alpha}}{\lambda_\ell}\mathrm{Im}\left[\frac{4\pi\chi_\ell^{(\alpha)}}{\Lambda_\ell}\right], \quad (7)$$

for $\ell = \{\pm, \|\}$, to the magnetic and density fluctuations through Maxwell's equations to obtain

$$\langle |B_\pm|^2\rangle = \frac{c^2 k_\parallel^2}{\omega^2}\langle |E_\pm|^2\rangle, \quad (8)$$

$$\langle |\rho|^2\rangle = \left(\frac{k_\parallel}{4\pi}\right)^2 \langle |E_\parallel|^2\rangle. \quad (9)$$

Here $B_\pm = (B_x \pm iB_y)/2$ represents the right-handed (left-handed) polarized magnetic field, n_α ($n_e = n_p \equiv n$) is the density of the species; $\omega_{p\alpha} = (4\pi n_\alpha q_\alpha^2/m_\alpha)^{1/2}$ and $\Omega_{c\alpha} = q_\alpha B_0/m_\alpha c$ are the plasma and cyclotron frequencies of species α, respectively; $\lambda_\pm = 1 - c^2k_\parallel^2/\omega^2$ and $\lambda_\parallel = 1$, respectively; and q_α ($q_p = -q_e$) is the charge of species α. $\Lambda_\pm$ and Λ_{zz} are the transverse and longitudinal (with respect to the background magnetic field) elements of the dispersion tensor for waves propagating parallel to the background magnetic field, given by

$$\Lambda_\pm = \lambda_\pm + 4\pi\sum_\alpha \chi_\pm^{(\alpha)}, \quad (10)$$

$$\Lambda_\parallel = \lambda_\parallel + 4\pi\sum_\alpha \chi_\parallel^{(\alpha)}. \quad (11)$$

The transverse $\chi_\pm^{(\alpha)}$ and longitudinal $\chi_\parallel^{(\alpha)}$ elements of the susceptibility of species α are given by Swanson (1989), Stix (1992), and Gomberoff et al. (2004)

$$\chi_\pm^{(\alpha)} = \frac{\omega_{p\alpha}^2}{4\pi\omega^2}\left[(1+A_\alpha) + \left(\xi_\alpha^{(0)} + (1+A_\alpha)\xi_\alpha^{(\pm)}\right)Z\left(\xi_\alpha^{(\pm)}\right)\right], \quad (12)$$

$$\chi_\parallel^{(\alpha)} = \frac{\omega_{p\alpha}^2}{2\pi k_\parallel^2 u_{\parallel\alpha}^2}\left[1 + \xi_\alpha^{(0)}Z\left(\xi_\alpha^{(0)}\right)\right], \quad (13)$$

where $A_\alpha = u_{\perp\alpha}^2/u_{\parallel\alpha}^2$ is a measure of the thermal anisotropy, $\xi_\alpha^{(\sigma)} = (\omega - k_\parallel U_\alpha + \sigma\Omega_\alpha)/(k_\parallel u_{\parallel\alpha})$, $\sigma = \{0, \pm\}$, and $Z(\xi)$ is the usual plasma dispersion function defined by Fried and Conte (1961). Hence, the magnetic and density fluctuations in magnetized plasmas depend on the dispersion tensor, which in turn depends on the macroscopic properties of the plasma.

For the case of electron–proton plasmas, it becomes useful to define the plasma $\beta_\parallel$ as

$$\beta = \beta_\parallel = 8\pi n\frac{T_\parallel}{B_0^2},$$

and the proton anisotropy as $A = T_\perp/T_\parallel$, where n is the particle number density, assumed equal for electrons and protons; and B_0 is the magnitude of the background field. It is convenient to define the normalized parameter

$$\frac{\omega_{pp}}{\Omega_c},$$

that characterizes the different space physics environments, and can affect the continuum spectrum produced by these fluctuations, which in turn may be used to understand the relevance of these processes occurring in a specific plasma environment. We consider a plasma composed of anisotropic non-drifting ($U_\alpha = 0$) protons and electrons. We also assume, for simplicity, that the electron parallel temperature equals that of the protons ($T_{\parallel e} = T_{\parallel p}$). We take the proton-to-electron mass ratio $m_p/m_e = 1836$ and first consider $\omega_{pp}/\Omega_c = 10^4$.

In Fig. 1(left) we show the spectrum $n\Omega_c\langle |B_-|^2\rangle/B_0^2$ produced by a solar wind type of plasma with $A = 1$ and $\beta_\parallel = 1$, for which the system is quasi-stable, as we will see below. The frequency has been normalized by Ω_c and the wave numbers by ω_{pp}/c. We note that the fluctuations produce a continuum spectrum, and can occupy a relevant part of the Fourier spectrum even in absence of free-energy for plasma instabilities. We also plot, as a reference, the normal modes of the system that are defined by $\det\Lambda_- = 0$, where we clearly see the Alfvén and cyclotron modes. Hence, theory and simulations produce quite similar results.

We can compare the result of Fig. 1(left) with an hybrid code (Terasawa et al., 1986; Navarro et al., 2014) that treats ions as particles and electrons as a massless charged neutralizing fluid. The code considers a 1D simulation box with 1024 grid cells, each containing 1000 particles, a system length of $251.3c/\omega_{pp}$, and a time step of $\Omega_c\Delta t = 0.02$.

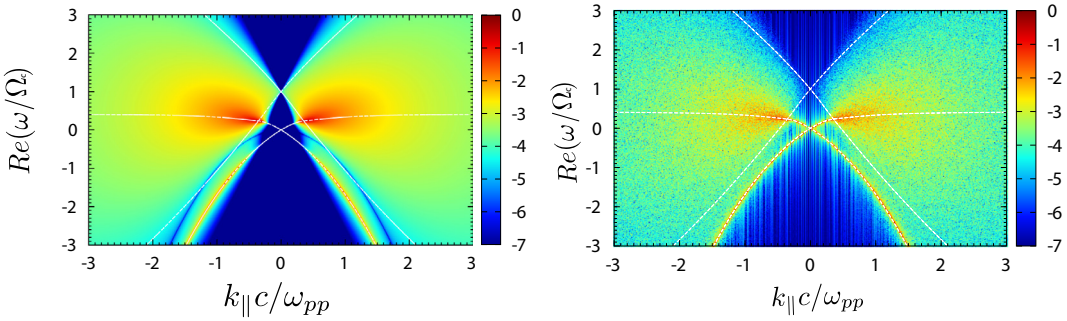

Fig. 1. The normalized spontaneous fluctuations spectra $n\Omega_e\langle|B_-|^2\rangle/B_0^2$ in the frequency and wavelength Fourier domain. Comparison between theory (left) and a hybrid simulation (right). We use a logarithmic (base 10) color coding, normalized to the maximum value for each case. The parameters are $A = 1.0$ and $\beta_\parallel = 1$. We use $\omega_{pp}/\Omega_e = 10^4$. The white lines corresponds to the normal modes of the system and the two less damped higher-order modes (HOM).

The boundary conditions are periodic for both particles and fields, and protons are loaded as a bi-Maxwellian distribution at $\Omega_e t = 0$. The simulation is constructed so that the parameters are equivalent to $A = 1$ and $\beta_\parallel = 1$. In Fig. 1(right) we display the spectrum from the simulation showing a close similarity with Fig. 1(left). The circularly polarized waves also become apparent in the simulation. The magnetic fluctuations are enhanced near the Alfvén-cyclotron mode, due to the denominator in Eq. (7), and they quickly lose their importance relative to the fluctuations for large values of $k_\parallel$.

To have a more global view of the relevance of thermally induced fluctuations, we define the total fluctuating magnetic energy density as

$$W_\pm = \frac{1}{8\pi}\int_{-\infty}^{\infty}\int_{-\infty}^{\infty} dk_\parallel d\omega \langle|B_\pm|^2\rangle, \tag{14}$$

and plot $(nc/\omega_{pp}B_0^2)W_-$ in the beta-anisotropy diagram (Fig. 2). We have restricted the calculation to regions far from the Alfvén cyclotron or firehose instabilities, so that we can claim that the plasma is close to a quasi-stable state.

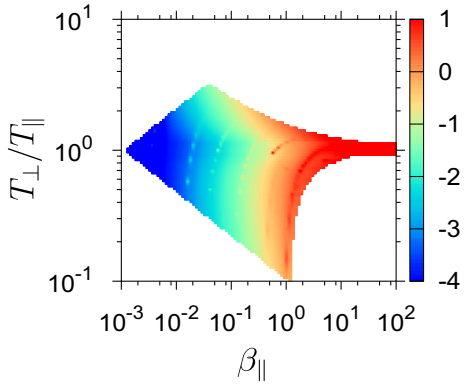

Fig. 2. Total fluctuating magnetic energy $(nc/\omega_{pp}B_0^2)W_-$ over the $\beta_\parallel - A$ plane as predicted by the theory. We use a logarithmic (base 10) color coding, normalized to the maximum value for each case. This Figure should be compared with the Fig. 1a of Bale et al. (2009). Although we can compute the total fluctuating magnetic energy for any value of $\beta_\parallel$ and A, we have restricted ourselves to $A > \beta_\parallel^{-1/3}/10$ and $A < \beta_\parallel^{1/3}/10$, where we do have solar wind measurements (see below).

This is done by calculating numerically the threshold value for instability through the dispersion relation and setting $\mathrm{Im}(\omega_{\max}/\Omega_e) = 10^{-3}$. Although we can compute the total fluctuating magnetic energy for any value of $\beta_\parallel$ and A, we have restricted ourselves to values for which there is solar wind data (see below) in the low $\beta_\parallel$ regime.

The magnetic energy is clearly enhanced near the instability thresholds, and its features are similar to solar wind observations near 1 AU, as reported in Fig. 1b of Bale et al. (2009). Hence the TIEF provides an alternative explanation to the observed magnetic variations in the solar wind (Navarro et al., 2014).

3. Variation with ω_{pp}/Ω_e

It is customary to organize the solar wind observations data in a beta-anisotropy diagram, as displayed in Fig. 3 (left), where we display the event probability distribution function $P(\beta, A)$, namely the number of solar wind observations for a given value of the proton β and proton A, measured by the Wind satellite (SWE 92-s) with a 1.5 min resolution for the year 2010, as obtained from the OMNI web page. In general for this period of time the satellite is at least 150 Earth radii in front of the Earth to reduce the effect of ion foreshocks, etc. The event probability is shown on a logarithmic scale in β and A with a bin size of 0.1 to ensure a good sampling for large and small parameter values, but properly accounting for the Jacobian of the transformation, so that $P(\beta, A)$ is really the event probability distribution function, but displayed in a logarithmic scale. Similarly, we display in Fig. 3(right) the average value over a given $\beta - A$ bin of the ratio ω_{pp}/Ω_e which characterizes the particular space plasma environment. For solar wind plasma, we can see a clear 2.5-order of magnitude variation ($10^3 \leqslant \omega_{pp}/\Omega_e \leqslant 10^{5.5}$) depending on the value β and A, but increasing with β. As a reference in the magnetosphere ω_{pp}/Ω_e can reach values close to 100.

In Fig. 4 we construct the fluctuation spectrum $\langle|B_-|^2\rangle$, for $A = 0.6$ and $\beta_\parallel = 0.1$, and varying values of the parameter ω_{pp}/Ω_e. We can note from Fig. 1 that, for these values

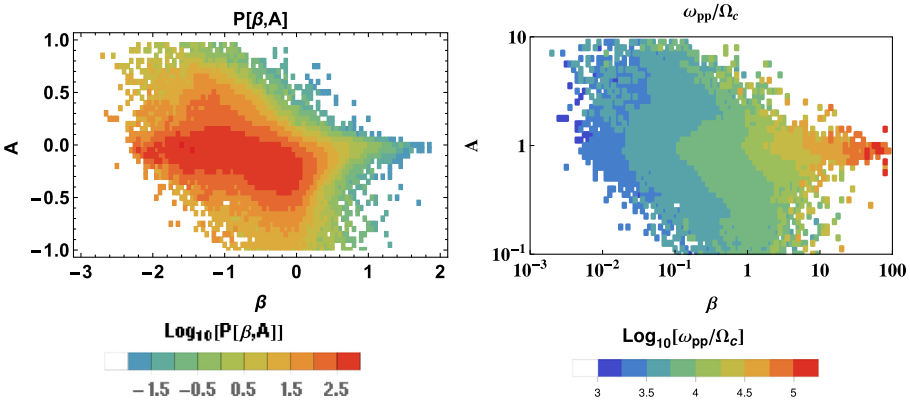

Fig. 3. (Left) Event probability distribution function $P(\beta, A)$ in the $\beta - A$ plane. (Right) The average value of ω_{pp}/Ω_c is displayed for each $\beta - A$ bin using a logarithmic color scale.

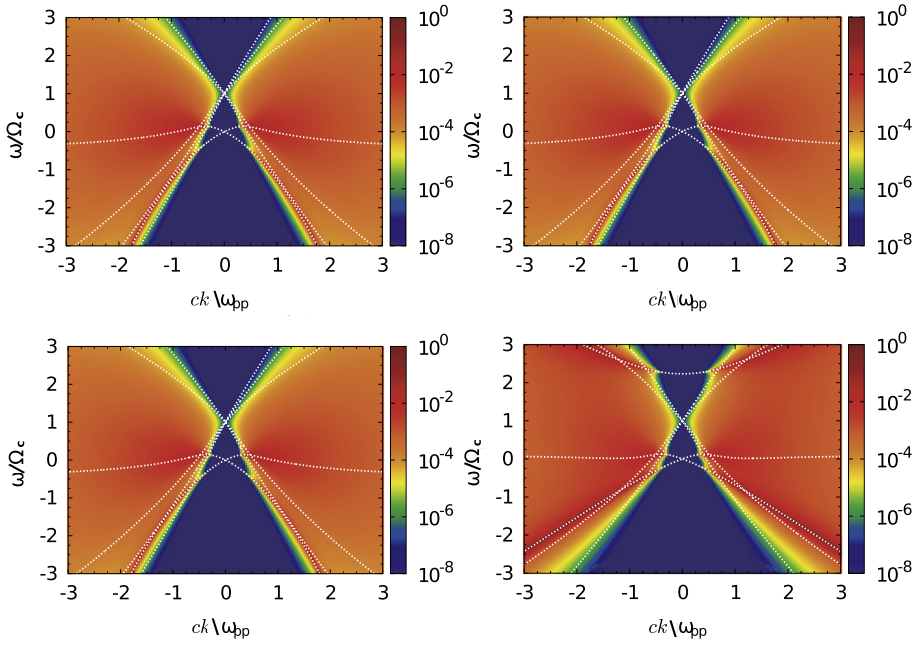

Fig. 4. Continuum fluctuation spectrum $n\Omega_c\langle|B_-|^2\rangle/B_0^2$ in the $\beta - A$ diagram for (top-left) $\omega_{pp}/\Omega_c = 10^3$, (top-right) $\omega_{pp}/\Omega_c = 10^2$, (bottom-left) $\omega_{pp}/\Omega_c = 10^1$, and (bottom-right) $\omega_{pp}/\Omega_c = 0.9^{-1}$. The parameters are $A = 0.6$ and $\beta_\parallel = 0.1$. We use a logarithmic (base 10) color coding, normalized to the maximum value for each case.

of A and $\beta_\parallel$, we are considering a quasi-stable situation. In particular in Fig. 4(top-left) we show the case $\omega_{pp}/\Omega_c = 10^3$ that applies to solar wind type plasmas. The values of ω and k for which $\Lambda_- = 0$ correspond to normal modes of the system that are the numerical solutions of the dispersion relation for transverse modes. We clearly see the usual fast/right-handed (third and fourth quadrants) and Alfvén-cyclotron modes (in the first and second quadrants). In the figure we also show a set of heavily damped modes crossing at $\omega/\Omega_c = 1$ known as quasi-modes or higher-order modes (HOM) (Astudillo, 1996). In general the damping of these modes increases with $k_\parallel$.

It is interesting to note that in general researchers disregard the HOMs because of their high damping rates, and concentrate on the undamped or slightly damped normal modes (Isenberg, 1984; Gomberoff and Elgueta, 1991; Thorne and Summers, 1991; Summers and Thorne, 1992; Hellberg and Mace, 2002; Xiao et al., 2007; Yoon et al., 2010; Mace and Sydora, 2010; Moya et al., 2013, 2014; Esfandyari-Kalejahi and Ebrahimi, 2014). For bi-Maxwellian plasmas, the HOM seems to constrain, in some qualitative way, the spectral region where the fluctuations seem to occur. Also, the HOMs structure is sorted by their damping in the bi-Maxwellian case. The least damped ones being the modes with frequencies ω closest to Ω_p and then their damping increases with their slopes.

In Fig. 4(top-right), (bottom-left), and (bottom-right), we consider the continuum spectrum $\langle|B_-|^2\rangle$ produced for

$\omega_{pp}/\Omega_c = 10^2$, 10, and 0.9^{-1}, respectively. The value of $\omega_{pp}/\Omega_c \sim 10^2$ corresponds to magnetospheric situations, and $\omega_{pp}/\Omega_c \leqslant 0.1$ may be applicable to astrophysical environments with large magnetic fields and low densities. It is important to mention that we have included these relatively low values ω_{pp}/Ω_c for completeness, however in these environments a treatment based on relativistic dynamics may be more appropriate (López et al., 2015). In general, it becomes of interest to note that as we decrease ω_{pp}/Ω_c the fluctuation spectrum become more relevant close to some of the HOM modes which interact with the previously called normal modes.

In Fig. 5 we construct the fluctuation spectrum $\langle|B_-|^2\rangle$, for $A = 0.6$ and $\beta_\parallel = 1.4$, and varying values of the parameter ω_{pp}/Ω_c, following the same trend as Fig. 4. We can note in Fig. 1 that, for these values of A and $\beta_\parallel$, we are considering a situation that is close to the firehose instability, and as such it produces a much higher level of fluctuations, as can be observed in the figures and noted in a number of references (Lund et al., 1996). It is interesting that as we decrease ω_{pp}/Ω_c the HOM also begin to interact with the previously called normal modes, and invade the spectral region of the fluctuations, specially for large k values.

4. Summary

Solar wind plasma are usually organized in the so called beta-anisotropy diagram, which shows that a large fraction of the plasma observations seem to be far below the instability thresholds, with an observable level of electromagnetic fluctuations. These fluctuations cannot be easily explained by linear theory due to the finite damping rate. Following Navarro et al. (2014), we propose that the fluctuations are produced by the balance between the electromagnetic fields generated by the thermal motion of the charged particles, which is consistent with the temperatures that define the particle distribution function; and the dissipation of the quasi-stable plasma. We have used the theory proposed by Navarro et al. (2014), constructed from the fluctuation–dissipation framework, to estimate the TIMF that would be produced in these anisotropic solar wind plasmas under quasi-stable conditions. This theory goes beyond linear theory and provides a possible explanation for the observed fluctuations, as seen in Fig. 2, which should be compared with Fig. 1a of Bale et al. (2009). The quasi-stable condition is defined for plasmas that have a small instability growth rate ($< 10^{-3}$), as compared with the other time scale of the system.

Although, the thermally induced fluctuations in a proton-electron plasma at the proton scale is normally characterized by $\beta_\parallel$ and the anisotropy A, there is a third parameter, namely ω_{pp}/Ω_c, that characterizes a particular space plasma environment. We have shown that the continuum spectrum of fluctuations change as we decrease ω_{pp}/Ω_c, strengthening the fluctuations close to the HOMs. The effect is more striking for a parameter range that may be more applicable to magnetospheric and astrophysics situations with large magnetic fields and low densities. We have included these relatively low values of ω_{pp}/Ω_c for completeness. Furthermore, it is important to mention that usually $\omega_{pp}/\Omega_c \sim 1$ appears in astrophysical settings

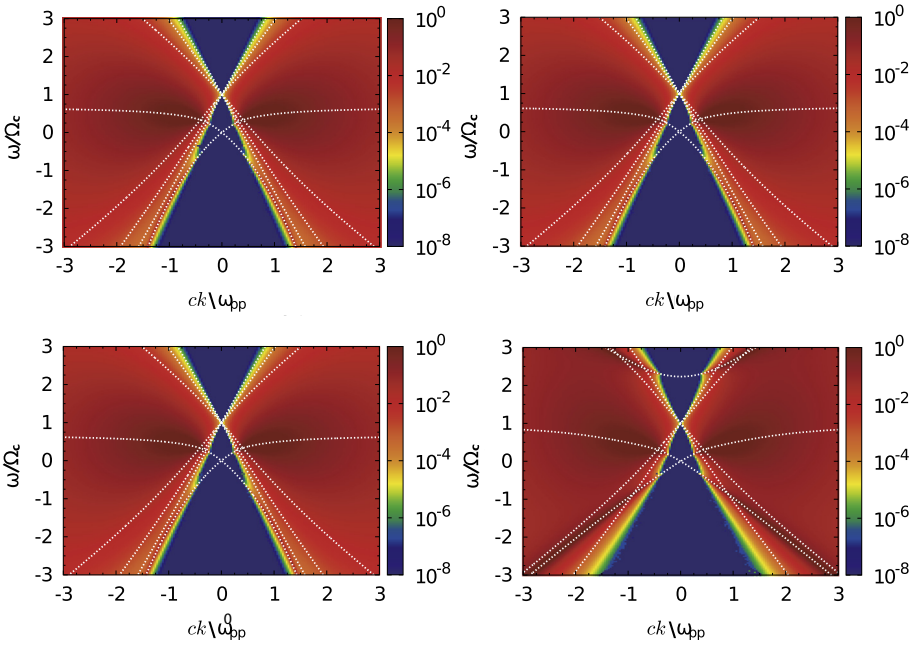

Fig. 5. Continuum fluctuation spectrum $n\Omega_c\langle|B_-|^2\rangle/B_0^2$ in the $\beta - A$ diagram for (top-right) $\omega_{pp}/\Omega_c = 10^2$, (bottom-left) $\omega_{pp}/\Omega_c = 10$, and (bottom-right) $\omega_{pp}/\Omega_c = 0.9^{-1}$. The parameters are $A = 0.6$ and $\beta_\parallel = 1.4$. We use a logarithmic (base 10) color coding, normalized to the maximum value for each case.

(López et al., 2015) where a relativistic treatment, with relativistic particle distribution functions, may be more appropriate.

The TIEF generally increase with β and become stronger as we get close to the instability threshold, as observed by comparing Figs. 4 and 5. Of course, beyond the instability threshold, the quasi-stable hypothesis breaks down and the theory cannot be applied, but under these conditions the plasma will evolve until it reaches a quasi-stable situation, if it is not forced. Of course, a large fraction of the solar wind observations are below the instability thresholds where the restrictions of quasi-stability, and hence the fluctuation–dissipation results, apply.

Acknowledgments

This project has been financially supported by FONDECyT under contracts No. 1150718 (J.A.V.), 1130273 (B.T.), 3150262 (R.E.N), 11150055 (P.S.M.), 1121144 (V.M.), 1161711 (V.M.). We also thank the support of CEDENNA and Conicyt Pia project ACT1405. We thank the support of VRIDEI/USACH under contract 041531SSSA_INTEXCELE (MS). A.F.V. thanks NASA's Grant NNX13AI65G and NASA's Wind/SWE mission for their support. We also are thankful for the WIND data obtained through the OMNI data base.

References

Araneda, J.A., Astudillo, H., Marsch, E., 2011. Interactions of Alfvén-cyclotron waves with ions in the solar wind. Space Sci. Rev. 172 (1–4), 361–372.

Astudillo, H.F., 1996. High-order modes of left-handed electromagnetic waves in a solar-wind-like plasma. J. Geophys. Res. 101 (A11), 24433–24442.

Bale, S., Kasper, J., Howes, G., Quataert, E., Salem, C., Sundkvist, D., 2009. Magnetic fluctuation power near proton temperature anisotropy instability thresholds in the solar wind. Phys. Rev. Lett. 103 (21), 211101.

Bruno, R., Carbone, V., Veltri, P., Pietropaolo, E., Bavassano, B., 2001. Identifying intermittency events in the solar wind. Planet. Space Sci. 49 (12), 1201–1210.

Callen, H.B., Welton, T., 1951. Irreversibility and generalized noise. Phys. Rev. 83, 34–40.

Camporeale, E., Passot, T., Burgess, D., 2010. Implications of a non-modal linear theory for the marginal stability state and the dissipation of fluctuations in the solar wind. Astrophys. J. 715 (1), 260–270.

Chapman, D.A., Gericke, D.O., 2011. Analysis of Thomson scattering from nonequilibrium plasmas. Phys. Rev. Lett. 107, 165004.

Davidson, R., Ogden, J.M., 1975. Electromagnetic ion cyclotron instability driven by ion energy anisotropy in high-beta plasmas. Phys. Fluids 18, 1045–1050.

Esfandyari-Kalejahi, A., Ebrahimi, V., 2014. Computation of generalized and exact dispersion relations for longitudinal plasma waves in nonextensive statistics and the effects of the nonextensivity on the oscillation modes and damps. Phys. Plasmas 21, 032126.

Fried, B.D., Conte, S.D., 1961. The Plasma Dispersion Function. Academic, San Diego, California.

Gary, S.P., Li, H., O'Rourke, S., Winske, D., 1998. Proton resonant firehose instability: temperature anisotropy and fluctuating field constraints. J. Geophys. Res. 103 (A7), 14567–14574.

Gary, S.P., McKean, M.E., Winske, D., Anderson, B.J., Denton, R.E., Fuselier, S.A., 1994. The proton cyclotron instability and the anisotropy/β inverse correlation. J. Geophys. Res. 99 (A4), 5903–5914.

Goldstein, M.L., Wicks, R.T., Perri, S., Sahraoui, F., 2015. Kinetic scale turbulence and dissipation in the solar wind: key observational results and future outlook. Phil. Trans. R. Soc. A 373, 20140147.

Gomberoff, L., Elgueta, R., 1991. Resonant acceleration of alpha particles by ion cyclotron waves. J. Geophys. Res. 96 (A6), 9801–9804.

Gomberoff, L., Muñoz, V., Valdivia, J.A., 2004. Ion cyclotron instability triggered by drifting minor ion species: cascade effect and exact results. Planet Space Sci. 52 (8), 679–684.

Hellberg, M.A., Mace, R.L., 2002. Generalized plasma dispersion function for a plasma with a kappa-Maxwellian velocity distribution. Phys. Plasmas 9 (5), 1495–1504.

Hellinger, P., Trávníček, P., Kasper, J.C., Lazarus, A.J., 2006. Solar wind proton temperature anisotropy: linear theory and WIND/SWE observations. Geophys. Res. Lett. 33 (9), L09101.

Ichimaru, S., 1962. Theory of fluctuations in a plasma. Ann. Phys. 20, 78–118.

Isenberg, P.A., 1984. The ion cyclotron dispersion relation in a proton-alpha solar wind. J. Geophys. Res. 89 (A4), 2133–2141.

Issautier, K., Moncuquet, M., Meyer-Vernet, N., Hoang, S., 2001. Quasi-thermal noise diagnostics in space plasmas. Astrophys. Space Sci. 277, 309–311.

Kasper, J., Lazarus, A., Gary, S., 2008. Hot solar-wind helium: direct evidence for local heating by Alfvén-cyclotron dissipation. Phys. Rev. Lett. 101 (26), 261103.

Kasper, J.C., Lazarus, A.J., Gary, S.P., 2002. Wind/SWE observations of firehose constraint on solar wind proton temperature anisotropy. Geophys. Res. Lett. 29 (17), 1839.

Li, B., Hazeltine, R.D., 2006. Applications of noise theory to plasma fluctuations. Phys. Rev. E 73, 065402.

López, R.A., Navarro, R.E., Moya, P.S., Viñas, A.F., Araneda, J.A., Muñoz, V.M., Valdivia, J.A., 2015. Spontaneous electromagnetic fluctuations in a relativistic magnetized electron-positron plasma. Astrophys. J. 810, 103.

Lund, E.J., LaBelle, J., Treumann, R.A., 1994. On quasi-thermal fluctuations near the plasma frequency in the outer plasmasphere: A case study. J. Geophys. Res. 99 (A12), 23651–23660.

Lund, E.J., Treumann, R.A., LaBelle, J., 1996. Quasi-thermal fluctuations in a beam-plasma system. Phys. Plasmas 3, 1234–1240.

Mace, R.L., Sydora, R.D., 2010. Parallel whistler instability in a plasma with an anisotropic bi-kappa distribution. J. Geophys. Res. 115 (A7), A07206.

Marsch, E., Goldstein, H., 1983. The effects of coulomb collisions on solar wind ion velocity distributions. J. Geophys. Res. 88 (A12), 9933–9940.

Meyer-Vernet, N., Couturier, P., Hoang, S., Steinberg, J.L., Zwickl, R.D., 1986. Ion thermal noise in the solar wind: Interpretation of the excess of electric noise on isee 3. J. Geophys. Res. 91 (A3), 3294–3298.

Meyer-Vernet, N., Hoang, S., Issautier, K., Moncuquet, M., Marcos, G., 2000. Plasma Thermal Noise: The Long Wavelength Radio Limit. Geophys. Monogr. Ser. 119, 67–74.

Moncuquet, M., Lecacheux, A., Meyer-Vernet, N., Cecconi, B., Kurth, W.S., 2005. Quasi thermal noise spectroscopy in the inner magnetosphere of saturn with cassini/rpws: Electron temperatures and density. Geophys. Res. Lett. 32 (20), L20S02.

Moya, P.S., Navarro, R.E., Viñas, A.F., Muñoz, V.M., Valdivia, J.A., 2014. Weak turbulence cascading effects in the acceleration and heating of ions in the solar wind. Astrophys. J. 781, 0245001.

Moya, P.S., Navarro, R., Muñoz, V.M., Valdivia, J.A., 2013. Comment on sensitive test for ion-cyclotron resonant heating in the solar wind. Phys. Rev. Lett. 111, 029001.

Navarro, R.E., Moya, P.S., Muñoz, V.M., Araneda, J.A., Viñas, A.F., Valdivia, J.A., 2014. Solar wind thermally induced magnetic fluctuations. Phys. Rev. Lett. 112, 245001.

Navarro, R.E., Moya, P.S., Muñoz, V.M., Araneda, J.A., Viñas, A.F., Valdivia, J.A., 2015. Magnetic Alfven-cyclotron fluctuations of

anisotropic non-thermal plasmas solar wind. J. Geophys. Res. 120, 2382–2396.
Navarro, R.E., Araneda, J., Muñoz, V.M., Moya, P.S., Viñas, A.F., Valdivia, J.A., 2014. Theory of electromagnetic fluctuations for magnetized multi-species plasmas. Phys. Plasmas 21, 092092.
Sagdeev, R., Shafranov, V., 1960. On the instability of a plasma with an anisotropic distribution of velocities in a magnetic field. Sov. Phys.–JETP 39, 181–184.
Schlickeiser, R., Yoon, P.H., 2012. Spontaneous electromagnetic fluctuations in unmagnetized plasmas I: General theory and nonrelativistic limit. Phys. Plasmas 19 (2), 022105.
Sentman, D.D., 1982. Thermal fluctuations and the diffuse electrostatic emissions. J. Geophys. Res.-Space 87 (A3), 1455–1472.
Seough, J., Yoon, P.H., Kim, K.-H., Lee, D.-H., 2013. Solar-wind proton anisotropy versus beta relation. Phys. Rev. Lett. 110, 071103.
Sitenko, A.G., 1967. Electromagnetic Fluctuations in Plasma. Academic, New York.
Štverák, Š., Trávníček, P., Maksimovic, M., Marsch, E., Fazakerley, A. N., Scime, E.E., 2008. Electron temperature anisotropy constraints in the solar wind. J. Geophys. Res. 113 (A3), A03103.
Stix, T.H., 1992. Waves in Plasmas. AIP, New York.
Summers, D., Thorne, R., 1992. A new tool for analyzing microinstabilities in space plasmas modeled by a generalized Lorentzian (kappa) distribution. J. Geophys. Res. 97 (A11), 827–832.
Swanson, D.G., 1989. Plasma Waves. Academic, San Diego.
Terasawa, T., Hoshino, M., Sakai, J., Hada, T., 1986. Decay instability of finite-amplitude circularly polarized Alfven waves – a numerical simulation of stimulated Brillouin scattering. J. Geophys. Res. 91, 4171–4187.
Thorne, R.M., Summers, D., 1991. Landau damping in space plasmas. Phys. Fluids B 3 (8), 2117–2123.
Viñas, A.F., Moya, P.S., Navarro, R.E., Valdivia, J.A., Araneda, J.A., Muñoz, V.M., 2015. Electromagnetic fluctuations of the whistler cyclotron and firehose instabilities in a Maxwellian and Tsallis-kappa-like plasma. J. Geophys. Res. 120, 3307–3317.
Weibel, E., 1959. Spontaneously growing transverse waves in a plasma due to an anisotropic velocity distribution. Phys. Rev. Lett. 2, 83–84.
Xiao, F., Zhou, Q., He, H., Zheng, H., Wang, S., 2007. Electromagnetic ion cyclotron waves instability threshold condition of suprathermal protons by kappa distribution. J. Geophys. Res. 112, A07219.
Yoon, P.H., Seough, J.J., Khim, K.K., Kim, H., Kwon, H.-J., Park, J., Park, S., Park, K.S., 2010. Analytic model of electromagnetic ion-cyclotron anisotropy instability. Phys. Plasmas 17, 082111.